

# PROGRESS ON SUPERCONDUCTING LINAC FOR THE RAON HEAVY ION ACCELERATOR

H. J. Kim\* representing the RAON, IBS, Daejeon, Korea

## Abstract

The RISP (Rare Isotope Science Project) has been proposed as a multi-purpose accelerator facility for providing beams of exotic rare isotopes of various energies. It can deliver ions from proton to uranium. Proton and uranium ions are accelerated upto 600 MeV and 200 MeV/u respectively. The facility consists of three superconducting linacs of which superconducting cavities are independently phased. Requirement of the linac design is especially high for acceleration of multiple charge beams. In this paper, we present the RISP linac design, the prototyping of superconducting cavity and cryomodule.

## INTRODUCTION

The RISP accelerator has been planned to study heavy ions in nuclear, material and medical science at the Institute for Basic Science (IBS). It can deliver ions from protons to uranium atoms with a final beam energy, for example, 200 MeV/u for uranium and 600 MeV for protons, and with a beam current range from 8.3 pμA (uranium) to 660 pμA (protons) [1, 2]. The facility consists of three superconducting linacs of which superconducting cavities are independently phased and operating at three different frequencies, namely, 81.25, 162.5 and 325 MHz.

## SUPERCONDUCTING LINAC

### Lattice Design

The configuration of the accelerator facility within the RISP is shown in Fig. 1. An injector system accelerates a heavy ion beam to 500 keV/u and creates the desired bunch structure for injection into the superconducting linac. The injector system comprises an electron cyclotron resonance ion source, a low-energy beam transport, a radio-frequency quadrupole, and a medium-energy beam transport. The superconducting driver linac accelerates the beam to 200 MeV/u. The driver linac is divided into three different sections, as shown in Fig. 2: a low-energy superconducting linac (SCL1), a charge stripper section (CSS) and a high-energy superconducting linac (SCL2). The SCL1 accelerates the beam to 18.5 MeV/u. The SCL1 uses two different families of superconducting resonators, i.e., a quarter wave resonator (QWR) and a half wave resonator (HWR). The SCL11 consists of 22 QWR's whose geometrical  $\beta$  is 0.047 and 22 quadrupole doublets. The resonance frequency of the QWR is 81.25 MHz. The cryomodule of the SCL11 hosts one superconducting cavity. The SCL12 consists of 102 HWR's whose geometrical  $\beta$  is 0.12 and 62 quadrupole doublets. The resonance frequency of the HWR

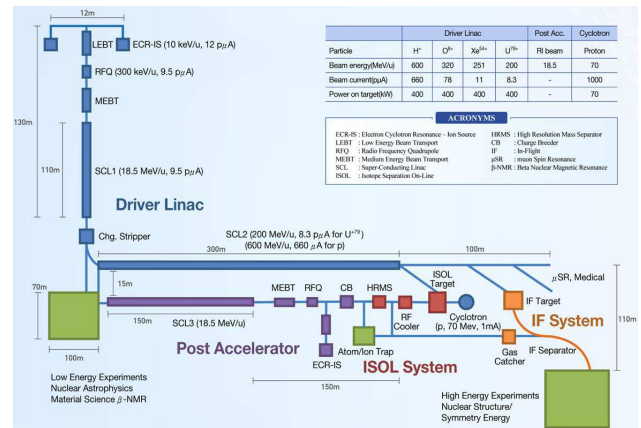


Figure 1: Layout of the RISP accelerator.

is 162.5 MHz. This segment has two families of cryomodules: one type of cryomodule hosts two superconducting cavities, and the other hosts four superconducting cavities. The CSS accepts beams at 18.5 MeV/u. The charge stripper strips electrons from the heavy-ion beams to enhance the acceleration efficiency in the high-energy linac section. The charge stripping section consists of normal conducting quadrupoles and room-temperature 45-degree bending magnets. The quadrupole magnets provide adequate transverse focusing and beam matching to the SCL2, and the bending magnet provides momentum dispersion for charge selection. The SCL2 accepts a beam at 18.5 MeV/u and accelerates it to 200 MeV/u. The SCL2 uses two types of single spoke resonators, i.e., SSR1 and SSR2. The SCL2 consists of the SCL21 and the SCL22, each with geometric  $\beta$  0.30, resonance-frequency 325-MHz SSR and a geometric  $\beta$  0.51, resonance-frequency 325-MHz SSR. The single-spoke-resonator type is chosen mainly because it can have a larger bore radius compared with the half-wave-resonator type, which is very important for reducing the uncontrolled beam loss in the high-energy linac section. The numbers of cavities in the SCL21 and the SCL22 is 69 and 138 respectively. The cryomodules of the SCL21 and SCL22 host 3 and 6 cavities, respectively. The SCL2 provides a beam into the in-flight fragmentation (IF) system via a high-energy beam transport (HEBT).

The post accelerator (SCL3) is designed to accelerate the rare isotopes produced in the ISOL (Isotope Separation On-Line) system. The SCL3 is, in principle, a duplicate of the driver linac up to low energy linear accelerator. The accelerated rare isotope beams are reaccelerated in the SCL2. Hence, the RISP accelerator provides a large number of rare isotopes with high intensity and with various beam energies.

\* hjkim@ibs.re.kr

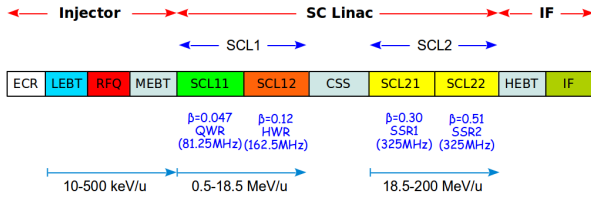


Figure 2: The RAON linear accelerator.

Table 1: Superconducting cavity parameters.

Parameter	Unit	QWR	HWR	SSR1	SSR2
Frequency	MHz	81.25	162.5	325	325
$\beta_g$		0.047	0.12	0.30	0.51
$L_{eff} = \beta_g \lambda$	m	0.173	0.221	0.277	0.452
$Q$	$10^9$	2.1	4.1	9.2	10.5
$QR_s$	$\Omega$	21	42	98	112
$R/Q$	$\Omega$	470	310	246	296
$E_{acc}$	MV/m	6.6	6.4	6.9	8.6
$E_{peak}/E_{acc}$		5.3	5.5	6.3	7.2
$B_{peak}/E_{acc}$	mT/(MV/m)	9.5	8.1	6.63	7.2

### Superconducting Cavity

In the optimization of the superconducting cavity, the resonant frequency, modes, and mechanical constraints in the cavity should be considered to design a high-efficient superconducting cavity. Figure of merits related with the cavity performance should be optimized. For particle beams passing through the cavity to get maximum energy gain, the acceleration gradient should be maximized while minimizing the peak electric and magnetic fields. Table 1 summarizes the parameters of four different superconducting cavities for the RISP superconducting linac. In order to achieve stable operation of the cavity, one of the critical issue is the multipacting effect inside of the cavity. It can cause damage to and external heating of the cavity. The multipactor effect is a phenomenon in which secondary electron emission occurs exponentially by electrons repeatedly hitting surface due to electron existing on the surface of the metal of the radio-frequency devices resonate with the RF electromagnetic field. Hence, the multipacting barriers of the QWR cavity are estimated with the secondary emission yield of 300°C-baked niobium. Several peaks are seen in the multipacting factors of four RF periods. The most serious multipactor occurs around the upper end of QWR at 1/8 the accelerating gradient. The detuning due to the tolerances of fabrication and the frequency sensitivities to mechanical deforming are estimated. The cavity is fabricated by using electron-beam welding of hydroformed 3-mm niobium sheets, drift tube and four additional ports. Two ports in the lower end are added for RF power and pickup coupling. The other two ports are installed for evacuation and high pressure rinsing. Figure 3 shows the prototype of quarter waver resonator. The detunings and the sensitivities of the bare cavity are shown in the Table 2. Figure 4 shows the result of measuring the Q-value versus acceleration electric



Figure 3: Quarter wave resonator after final electron beam welding.

Table 2: Frequency shift due to various sources.

Frequency shift	Value (MHz)
Resonant frequency	81.25
External pressure (130 kPa)	81.27
Cool down (293 K → 4 K)	81.27
Vaccum	81.068
BCP (150 $\mu$ m)	81.069
Welding shrinkage (0.6 mm)	80.898
Clamp-up test	80.855

field ( $E_{acc}$ ) for QWR cavity [3]. Normally, we cool down the cavity fast from room temperature to 4 K. The duration between 150 K and 4 K is around 25 minutes. In a measurement of 4K-1st and 4K-2nd, low-temperature (120°C) baking is not applied. After baking the cavity at 120°C, the Q-factor is improved twice at  $E_{acc} = 6.6$  MV/m. In order to check the Q-disease effect, the cavity spends 7.5 hr in the Q-disease temperature window (50 K to 100 K). The 4K-QD in Fig. 4 shows the Q-disease performance and indicates some measure of hydrogen in the cavity. The performance reduction due to Q-disease is nearly recovered by a 250 K thermal cycle. The residual resistance is measured to be 2.5

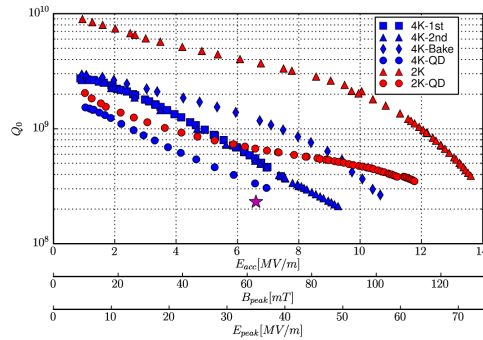


Figure 4: Measurement of Q-value of quarter wave resonator.

Table 3: Thermal load (Watt at 4.5K) of superconducting linacs.

	SCL11	SC12	SCL21	SCL22	SCL31	SCL33
Dynamic	532	2,016	1,014	5,009	532	2,016
Static	227	1,071	475	790	227	1,071
Sum	760	3,087	1,489	5,800	760	3,087

nΩ. The maximum accelerating gradient achieved at 2 K is 13.6 MV/m without quench corresponding to an equivalent peak electric field of 72 MV/m and a peak magnetic field of 129 mT.

### Cryomodule

The linac has five types of cryomodules for four different kinds of cavities [4]. The main roles of the cryomodules are maintaining the operating condition of the superconducting cavities and aligning the cavities along the beam line. A high level of vacuum and thermal insulation are required for the cryomodule to maintain the operating temperature of the superconducting cavities. The cryomodules hosting the QWR and the HWR cavities are box-type while those hosting the SSR1 and the SSR2 cavities are cylindrical. Both QWR and HWR cavities are vertically installed in the cryomodule. The main components of the cryomodule are dressed cavities, two-phase pipe, power couplers to supply RF power to the cavities, tuners to control the operation of the cavities, and support systems to fix the cavities along the beam line. Because the operating temperature of the superconducting cavities are 2 K, 40-K and 4.5-K thermal intercepts are installed to minimize the thermal load. The cold mass, including the cavity string, coupler and tuner, is installed on a strong back and is then inserted into a vacuum vessel with a thermal shield and a multi-layer insulator. The thermal loads of the superconducting linacs are summarized in Table 3. The dynamic and the static loads are 70% and 30% of the total thermal load, respectively. The designs of the cryomodule components have been conducted based on thermal and structural concerns. The thermal design starts by the estimating of the thermal loads that determine the required sizes of components such as the two phase pipes and the other cryogenic pipes. Three levels of cryogenic flow are necessary: 2 K, 4.5 K and 70K. Figure 5 shows the prototype of quarter wave resonator cryomodule and P&ID diagram of cryogenic system. The static heat load is measured for QWR cryomodule. The helium flow rate and static thermal load versus time are shown in Fig. 6. The design and measured static loads are 4W and 3.9 W respectively.

### SUMMARY

The RISP linacs have been presented. In the design, four different cavities, QWR, HWR, SSR1 and SSR2, were used to accelerate the beam in the linac. The number of cavities per cryomodule at each section was optimized to minimize

the total number of cavities required for efficient accelera-

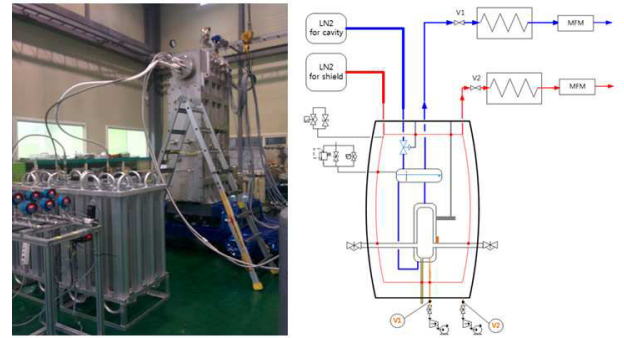


Figure 5: Prototype of quarter wave resonator cryomodule and P&ID.

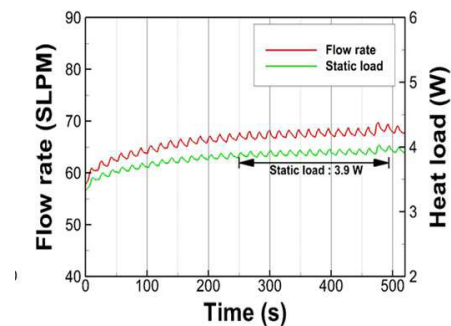


Figure 6: Measurement of static thermal load of quarter wave resonator cryomodule.

tion. We emphasized the stability of operation, the flexibility of maintenance, and the minimization of beam loss. The prototype of superconducting cavities have been fabricated and tested in the cryogenic temperature. The result shows that the target value of Q-factor is achieved with a margin. The box-shaped and cylindrical cryomodules are designed for hosting cavities. The testing of the cryomodules is under way.

### ACKNOWLEDGMENTS

This work was supported by the Rare Isotope Science Project which is funded by the Ministry of Science, ICT and Future Planning (MSIP) and the National Research Foundation (NRF) of the Republic of Korea under Contract 2011-0032011.

### REFERENCES

- [1] S. K. Kim, Rare Isotope Science Project: Baseline Design Summary (2012).
- [2] D. Jeon, et. al., in *Proceedings of LINAC2012*, TUPB030 (2012) p. 540.
- [3] Z. Y. Yao, et. al., RISP QWR Initial Cold Test Report (2014).
- [4] W.K. Kim et al, in *Proceedings of IPAC15*, WEPMN035 (2015).